DE GRUYTER Pure Appl. Chem. 2020; 92(7): 1081–1092

Conference paper

Anastasia M. Cheplakova, Denis G. Samsonenko and Vladimir P. Fedin*

Octafluorobiphenyl-4,4′-dicarboxylate as a ligand for metal-organic frameworks: progress and perspectives

https://doi.org/10.1515/pac-2019-1210

Abstract: While metal-organic frameworks based on aromatic carboxylates are very numerous and well investigated, the chemistry of their fully fluorinated analogues is at the very beginning. This minireview aims at summarizing all metal complexes with octafluorobiphenyl-4,4′-dicarboxylate (oFBPDC^{2-}) anion and in particular, porous coordination polymers, their syntheses, crystal structures and functional properties highlighting the importance of further investigation of such systems.

Keywords: gas sorption; hydrophobicity; Mendeleev-21; metal-organic frameworks; perfluorinated ligands; photoluminescence.

Introduction

Metal-organic frameworks or porous coordination polymers (MOFs, PCPs) are compounds consisting of metal ions or clusters linked with organic ligands to form a coordination framework. These compounds contain cages or cavities, i.e. they are porous materials and could be utilized in different applications: gas sorption and separation, heterogeneous catalysis as well as nanoreactors, sensing, electron and ionic conductivity, energy, and environmental applications [1–5]. The most exciting features of MOFs compared to other porous materials are broad possibilities of design and modification of the framework structure and topology, internal surface and porosity for a certain application or industrial challenges. The most famous MOFs, IRMOF [6], MIL [7–10], UiO [11] series, are formed by anions of aromatic dicarboxylate ligands, e.g. terephthalate 1,4-BDC^{2-}. The use of their perfluorinated analogues tFBDC^{2-} potentially leads to a material with new properties or enhanced characteristics. For instance, the intensity of near-infrared luminescence of Er(III) is 3 times higher for complex with perfluorinated ligand 1,4-tFBDC then with BDC^{2-} [12]. The ligand fluorination improves both framework stability and sorption capacities towards H_2 and CO_2 which was shown on isostructural series of MOFs built up with Ni(II), 2,4,6-tri(4-pyridyl)-1,3,5-triazine, and substituted phthalate 1,2-BDC^{2-} [13]. Perfluorinated In(III) framework YCM-101 is suggested for the removal of antibiotics from water solutions

---

Article note: A collection of invited papers based on presentations at 21st Mendeleev Congress on General and Applied Chemistry (Mendeleev-21), held in Saint Petersburg, Russian Federation, 9–13 September 2019.

***Corresponding author: Vladimir P. Fedin,** Nikolaev Institute of Inorganic Chemistry, Siberian Branch of the Russian Academy of Sciences, 3 Acad. Lavrentiev Ave., Novosibirsk 630090, Russian Federation; and Novosibirsk State University, 2 Pirogova Str., Novosibirsk 630090, Russian Federation, e-mail: cluster@niic.nsc.ru
Anastasia M. Cheplakova and Denis G. Samsonenko: Nikolaev Institute of Inorganic Chemistry, Siberian Branch of the Russian Academy of Sciences, 3 Acad. Lavrentiev Ave., Novosibirsk 630090, Russian Federation; and Novosibirsk State University, 2 Pirogova Str., Novosibirsk 630090, Russian Federation

© 2020 IUPAC & De Gruyter. This work is licensed under a Creative Commons Attribution-NonCommercial-NoDerivatives 4.0 International License. For more information, please visit: http://creativecommons.org/licenses/by-nc-nd/4.0/

[14]. Other examples of fluorine-containing MOF structures and their properties are summarized in review [15] and book chapter [16].

A further step toward a highly porous fluorinated framework is the use of longer bridging perfluorinated ligand octafluorobiphenyl-4,4′-dicarboxylate oFBPDC^{2-}. However oFBPDC-containing coordination polymers are extremely scarce, they do demonstrate intriguing functional properties, including gas sorption, hydrophobicity, etc. In this review, we summarize all the achievements concerning oFBPDC^{2-} chemistry in terms of the formation of metal complexes and especially those showing permanent porosity, and their properties.

The synthesis of H_2oFBPDC

One of the key factors that hinder the development of oFBPDC^{2-} coordination chemistry is the accessibility of this ligand for chemists. Unlike tetrafluoroterephthalic acid and its isomers, perfluorinated biphenyl-4,4′-dicarboxylic acid is not a commercially available chemical. There are some protocols allowing one to get this substance in up to 10 g quantity in a few stages. The major transformation involves the C–C coupling reaction between the derivatives of fluorinated benzoic acid: Cu-catalyzed cross-coupling reaction between 2,3,5,6-tetrafluorobenzonitrile and 2,3,5,6-tetrafluoro-4-iodobenzonitrile [17] (Scheme 1a) and a coupling reaction of (4-ethoxy-carbonyl-2,3,5,6-tetrafluorophenyl)zinc in the presence of anhydrous $CuCl_2$ [18] (Scheme 1b). Further hydrolysis of dinitrile (Scheme 1a) or diester leads to octafluorobiphenyl-4,4′-dicarboxylic acid (Scheme 1b). The synthetic routes with some slight modifications were also performed [19, 20].

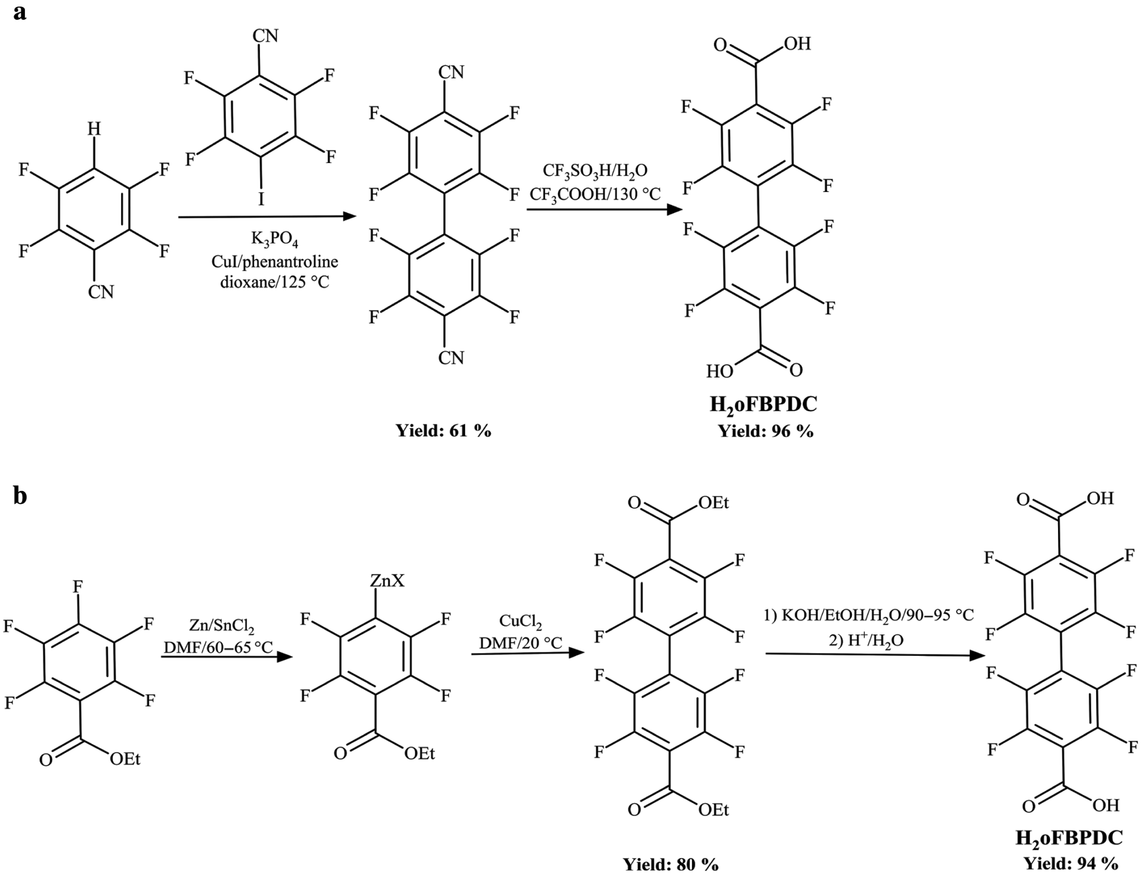

Scheme 1: Syntheses of H_2oFBPDC.

Metal complexes containing oFBPDC^{2-}

All metal complexes containing oFBPDC^{2-} are summarized in Table 1. The first MOFs based on oFBPDC^{2-} are Cu-containing MOFF-1 and MOFF-2 which have been published in 2013 by the group of prof. Miljanić [17]. The idea of using a fully fluorinated linker is to combine advantages of MOF materials with exceptional hydrophobicity of fluorinated organic polymers and its increased stability toward moisture. Both MOFF-1 and MOFF-2 are synthesized at 40–60 °C in the mixture of solvents in which methanol is a major component. MOFF-1 is a layered coordination polymer built up with binuclear paddle wheel units $\{Cu_2(RCO_2)_4L_2\}$ and bridging oFBPDC^{2-}, with methanol as an apical ligand L. These square grid layers can be pillared with bridging N-donor ligand dabco (dabco – 1,4-diazabicyclo[2.2.2]octane) to form doubly interpenetrated 3D coordination polymer. Owing to the presence of F atoms within the organic ligand, desolvated MOFF-1 and MOFF-2 do demonstrate hydrophobic and superhydrophobic behavior. Water contact angles of MOFF-1 and MOFF-2 were $108 \pm 2°$ and $151 \pm 1°$.

The authors [17] highlighted that the synthesis of MOFs based on this perfluorinated ligand occurred at much lower temperatures than the conventional solvothermal synthesis of non-fluorinated congeners. The reason for this is the higher acidity of H_2oFBPDC in comparison with H_2BPDC. The difference in K_a values in water solutions of aromatic perfluorinated/non-fluorinated acids is 2–3 orders of magnitude [21, 22]. Higher acidity of the reaction mixture may prevent the formation of the metal complexes with polycarboxylate ligands since they are usually not stable under strongly acidic conditions. In this regard, Cheetham and coworkers suggested that the formation of the polymeric structures with perfluorinated benzenedicarboxylates easily took place in the presence of N-containing ligands which acted both as a co-ligand and a base [23]. On the other hand, higher acidity of H_2oFBPDC allows one to use metal hydroxides as metal sources. In this particular case, the reaction between starting materials represents not only a complexation reaction but also a neutralization one. This approach appeared to be very productive in the case of some lanthanides and zinc complexes. Thus, in 2015 Larionov et al. described the syntheses and photoluminescence properties of novel Tb(III) and Eu(III) complexes – $Ln_2(H_2O)_4(oFBPDC)_3 \cdot 3H_2O$ and $Ln_2(phen)_2(oFBPDC)_3 \cdot 2H_2O$. These complexes have been obtained by the reaction of $Ln(OH)_3$, H_2oFBPDC and phen (phen = 1,10-phenantroline) in water at room temperature with further precipitation with acetone/methanol solvent mixture [18]. Though these complexes have not been structurally characterized, they are supposed to be polymeric. Photoluminescence spectra of all four lanthanide complexes contain narrow bands which are assigned to transitions in Tb^{3+} and Eu^{3+} cations. In 2019, the same group has reported the synthesis and X-ray crystallography data for $[Zn(H_2O)_6][Zn(H_2O)_4(oFBPDC)_2] \cdot H_2O$ having the non-polymeric structure [24]. Interestingly, each oFBPDC^{2-} is linked to Zn(II) cation by means of only one carboxylate group coordinated in monodentate mode. There is a complicated system of hydrogen bonding interactions between non-coordinated O atoms of fluorinated dicarboxylates, lattice and coordinated water molecules (Fig. 1).

In our investigation of the Zn(II) + oFBPDC^{2-} system in terms of the formation of metal complexes we managed to obtain 12 novel Zn complexes of non-polymeric ionic, 1D, 2D and 3D structures [20, 25]. $Zn(NO_3)_2 \cdot 6H_2O$, $Zn(CH_3COO)_2 \cdot 2H_2O$, and freshly prepared $Zn(OH)_2$ have been used as metal source. The syntheses took place in water, alcohols and their derivatives, acetone, acetonitrile, tetrahydrofurane (THF), *N,N*-dimethylformamide (DMF), *N,N*-dimethylacetamide (DMA), *N,N*-diethylformamide (DEF) and dimethylsulfoxide (DMSO) in the range of temperatures from room temperature up to 100 °C. In some cases, N-donor co-ligands (4,4′-bipyridile (bpy), dabco, urotropine (ur)) were added. Dabco and bpy with a linear arrangement of nitrogen atoms are often used for the construction of porous MOFs. Due to the presence of four nitrogen atoms in ur and their angular arrangement this ligand can act as a four, three-, or two-connected linker [26] as well as a terminal ligand [27].

Extensive perfluorination of the carboxylic acid not only changes the reactivity (e.g. acidity, thermal stability [28]) but also electronic properties of the carboxylate. oFBPDC^{2-} is expected to be a weak ligand. Indeed, the reaction of $Zn(CH_3COO)_2 \cdot 2H_2O$, H_2oFBPDC and dabco in DMF in a sealed tube at 60 °C afforded single crystals which appeared to be $[Zn_2(CH_3COO)_3(OH)(dabco)]$ [29], which did not contain oFBPDC^{2-}. Besides, we failed to get any metal complexes in DMF, DEF, DMSO, while the use of the solvents with lower

Table 1: The summary of oFBPDC-containing metal complexes.

Metal	Chemical formula	Starting materials and synthetic conditions	Dimensionality	Investigated properties	Ref
Cu	$[Cu_2(CH_3OH)_2(oFBPDC)_2]\cdot 2CH_3OH$ (MOFF-1)	$Cu(NO_3)_2\cdot 2.5H_2O$, $H_2oFBPDC$, 1:1 molar ratio $CH_3OH/DMF/H_2O$ (v:v:v = 18:1:1), 40 °C, 4 days	2D	Porosity and hydrophobicity	[17]
	$[Cu_2(dabco)(oFBPDC)_2]$ (MOFF-2)	$Cu(NO_3)_2\cdot 2.5H_2O$, $H_2oFBPDC$, dabco 2:2:1 molar ratio $CH_3OH/DMF/H_2O$ (v:v:v = 20:3.33:1), 60 °C, 2 days	3D		
Ln = Tb, Eu	$[Ln_2(H_2O)_4(oFBPDC)_3]\cdot 3H_2O$	$Ln(OH)_3$, $H_2oFBPDC$, 2:3 molar ratio	N/D[a]	Photoluminescence	[18]
	$[Ln_2(phen)_2(oFBPDC)_3]\cdot 2H_2O$	$Ln(OH)_3$, $H_2oFBPDC$, phen · H_2O, 2:3:2 molar ratio dissolution in water at room temperature with further precipitation by adding acetone/CH_3OH mixture (v:v = 3:1)	N/D[a]		
Zn	$[Zn(eg)_3](oFBPDC)$	$Zn(OH)_2$, $H_2oFBPDC$, 1:1 molar ratio eg, 40 °C, 48 h	0D	–	[20]
	$[Zn(H_2O)_6][Zn(H_2O)_4(oFBPDC)_2]\cdot H_2O$	$Zn(CH_3COO)_2\cdot 2H_2O$, $H_2oFBPDC$ 1:1 molar ratio C_2H_5OH, full evaporation with further recrystallization from H_2O, room temperature	0D	–	[24]
	$[Zn(H_2O)(ur)(oFBPDC)]$	$Zn(OH)_2$, $H_2oFBPDC$, ur, 1:1:1 molar ratio C_2H_5OH, 20–60 °C, 3 months	1D	–	[20]
	$[Zn(CH_3OH)_2(CH_3OCH_2CH_2OH)(oFBPDC)]$	$Zn(OH)_2$, $H_2oFBPDC$, 1:1 molar ratio CH_3OH/2-methoxyethanol (v:v = 1:1), 40 °C, 72 h	1D	–	[20]
	$[Zn(CH_3OH)_3(ur)(oFBPDC)]$	$Zn(OH)_2$, $H_2oFBPDC$, ur, 1:1:1 molar ratio CH_3OH, 40 °C, 24 h	1D	–	[25]
	$[Zn_2(CH_3CONH_2)_2(oFBPDC)_2]\cdot 3CH_3CN$	$Zn(NO_3)_2\cdot 6H_2O$, $H_2oFBPDC$, CH_3CONH_2 1:1:1 molar ratio CH_3CN, 80 °C, 40 h	2D	Porosity	[25]
	$[Zn(CH_3OH)_3(oFBPDC)]$	$Zn(OH)_2$, $H_2oFBPDC$, 1:1 molar ratio CH_3OH, 60 °C, 24 h	2D	–	[25]
	$[Zn_2(CH_3CN)_2(oFBPDC)_2]\cdot 2C_6H_6\cdot 2CH_3CN$	$Zn(NO_3)_2\cdot 6H_2O$, $H_2oFBPDC$, 1:1 molar ratio CH_3CN/C_6H_6 (v:v = 2:1), 80 °C, 48 h	2D	Porosity	[20]
	$[Zn_2(H_2O)_2(oFBPDC)_2]\cdot 4(CH_3)_2CO$	$Zn(OH)_2$, $H_2oFBPDC$, 1:1 molar ratio acetone, H_2O (v:v = 2:1), 40 °C, 10 days	2D		[20]

Table 1 (continued)

Metal	Chemical formula	Starting materials and synthetic conditions	Dimensionality	Investigated properties	Ref
	$[\{Zn_4(\mu_3\text{-}CH_3O)_4\}(CH_3OH)_4(oFBPDC)_2] \cdot [\{Zn_4(\mu_3\text{-}CH_3O)_4\}(H_2O)(CH_3OH)_3(oFBPDC)_2] \cdot 13CH_3OH$	$Zn(OH)_2$, $H_2oFBPDC$ CH_3OH/eg (v:v = 30:1), 60 °C, 3 weeks	2D	–	[20]
	$[Zn_2(H_2O)_{1.5}(thf)_{1.5}(oFBPDC)_2] \cdot 3.5H_2O \cdot 2.5THF$	$Zn(OH)_2$, $H_2oFBPDC$, 1:1 molar ratio THF, 40 °C, 6 days	3D	Porosity	[25]
	$[Zn_2(dabco)(oFBPDC)_2] \cdot 4.5CH_3OH$	$Zn(OH)_2$, $H_2oFBPDC$, dabco, 2:2:1 molar ratio CH_3OH, 80 °C, 48 h	3D	Porosity, hydrophobicity	[25]
	$(H_2bpy)[Zn_2(bpy)(oFBPDC)_3]$	$Zn(OH)_2$, $H_2oFBPDC$, bpy, 2:3:2 molar ratio H_2O, 70 °C, 72 h	3D	Hydrophobicity	[25]
Zr	$Zr_6O_4(OH)_4(oFBPDC)_{4.27}[(OH)(OH_2)]_{3.46}$	$ZrOCl_2 \cdot 8H_2O$, $H_2oFBPDC$, 1:1 molar ratio THF/$HCl_{conc.}$ (v:v = 96:1), 80 °C, 24 h	3D	Porosity, Lewis acidity of Zr centres	[19]

[a] No crystallographic data.

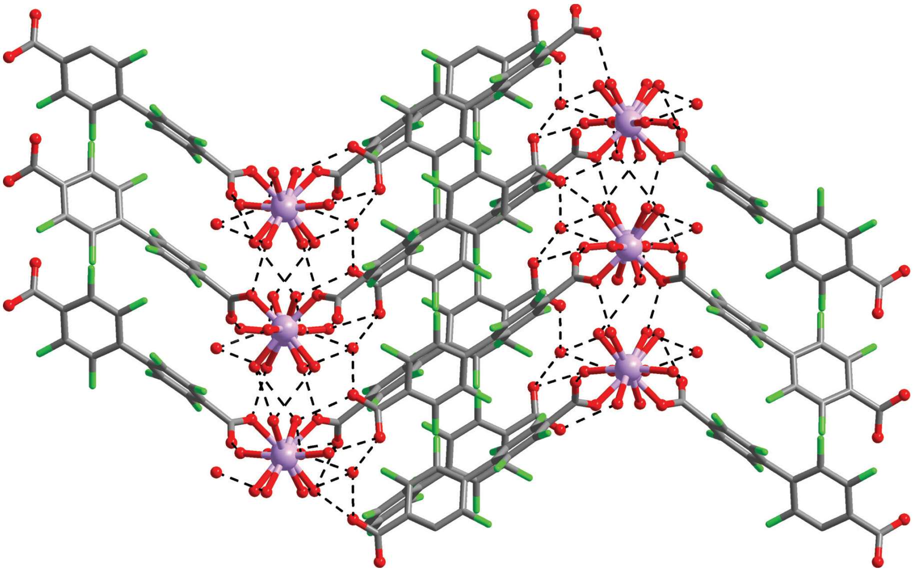

Fig. 1: Fragment of the crystal packing in $[Zn(H_2O)_6][Zn(H_2O)_4(oFBPDC)_2] \cdot H_2O$. Hydrogen bonding interactions are shown with dashed lines. Hydrogen atoms are omitted for clarity.

donor ability proved to be very productive. The reaction of $Zn(OH)_2$ with H_2oFBPDC in ethylene glycol (eg) lead to non-polymeric complex $[Zn(eg)_3]$(oFBPDC) [20] however the similar reaction of $Sc(OH)_3$ with tetrafluoroterephthalic acid gave a chain-like polymer [30]. In this complex, oFBPDC^{2-} acts as a counter-ion and is not bounded to Zn(II) cation. This complex is expected to be a convenient source for the synthesis of novel oFBPDC based MOFs. The investigation of its reactivity is underway. The reaction of $Zn(OH)_2$ and H_2oFBPDC in the mixture of solvents 2-methoxyethanol/methanol at 40 °C produced 1D coordination polymer $[Zn(CH_3OH)_2(CH_3OCH_2CH_2OH)(oFBPDC)]$ [20]. The interaction of $Zn(OH)_2$, H_2oFBPDC and ur in 1:1:1 molar ratio produced different chain-like coordination polymers depending on the solvent (Fig. 2). The reaction in methanol gave $[Zn(CH_3OH)_3(ur)(oFBPDC)]$ (Fig. 2a) [25], while the reaction in ethanol produced $[Zn(H_2O)(ur)(oFBPDC)]$ (Fig. 2b) [20]. In the former coordination polymer, a distorted octahedral coordination environment of Zn(II) is presented by two O atoms of carboxylates, one N atom of terminal ur, and three O atoms of methanol molecules. In the crystal structure of the latter compound, each Zn(II) cation has a distorted tetrahedral environment consisting of two O atoms of carboxylates, one N atom of terminal ur, and one O atom of water.

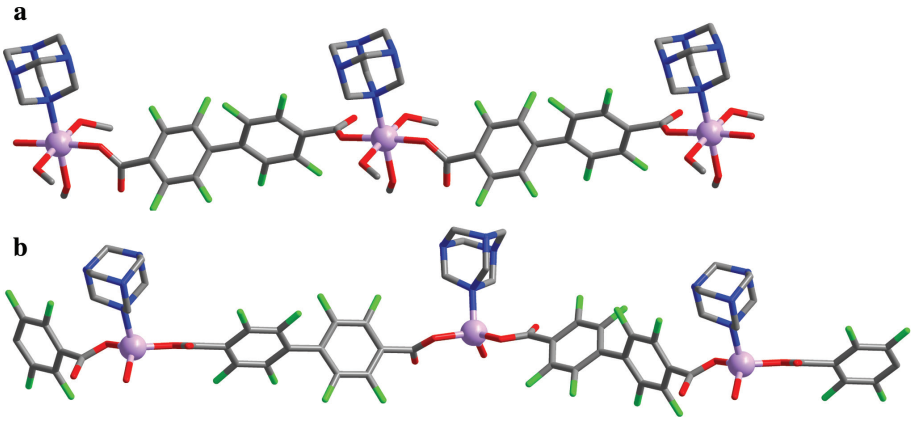

Fig. 2: Fragments of the polymeric chains of $[Zn(CH_3OH)_3(ur)(oFBPDC)]$ (a) and $[Zn(H_2O)(ur)(oFBPDC)]$ (b). Hydrogen atoms are omitted for clarity.

Among 2D coordination polymers is [Zn(CH_3OH)$_3$(oFBPDC)] [25] which is obtained in the reaction of Zn$(OH)_2$ and H_2oFBPDC in methanol in the range 40–60 °C. Interestingly, if a small amount of eg (~3 vol.%) is added to the same reaction mixture, the product of the reaction after prolonged heating at 60 °C represents non-identified powder and large crystals of layered coordination polymer [{Zn_4(μ_3-OCH_3)$_4$}(CH_3OH)$_4$(oFBPDC)$_2$] ·[{Zn_4(μ_3-OCH_3)$_4$}(H_2O)(CH_3OH)$_3$(oFBPDC)$_2$] · 13CH_3OH [20]. Each layer of this polymer is built up with unique cuboidal coordination fragment {Zn_4(μ_3-OCH_3)$_4$}. This unit is found in organometallic compounds, obtained by the controlled oxidation of zinc alkyls [31–33], but not in Zn coordination polymers. To the best of our knowledge, such a 2D coordination polymer is the first example of Zn coordination polymers based on {Zn_4(μ_3-OCH_3)$_4$} units and carboxylate linkers. Complex [Zn_2(CH_3CONH_2)$_2$(oFBPDC)$_2$] · 3CH_3CN [25] having layered polymeric structure is the first coordination polymer we managed to obtain by the reaction of Zn$(NO_3)_2$ · 6H_2O and H_2oFBPDC in CH_3CN after *ca.* 5 days at 80 °C. The complex contains acetamide as an apical ligand L within paddle wheel fragment {Zn_2(RCO_2)$_4$$L_2$}. Acetamide presumably arises from the acid-catalyzed hydrolysis of CH_3CN. If a similar reaction takes place in the mixture of solvents CH_3CN/benzene (v:v = 2:1) at 80 °C, another coordination polymer [Zn_2(CH_3CN)$_2$(oFBPDC)$_2$] · 2C_6H_6 · 2CH_3CN [20] with similar layered structure is formed within 2 days. Due to rapid crystallization, there is no acid-catalyzed hydrolysis, and CH_3CN is coordinated to Zn(II) cations in contrast to CH_3CONH_2 in [Zn_2(CH_3CONH_2)$_2$(oFBPDC)$_2$] · 3CH_3CN. Guest molecules of benzene take part in π-π interactions with fluorine substituted phenyl rings. The same square grid layers formed with Zn paddle wheels {Zn_2(RCO_2)$_4$$L_2$} and oFBPDC^{2-} are found in the crystal structure of [Zn_2(H_2O)$_2$(oFBPDC)$_2$] · 4CH_3COCH_3 [20]. This layered coordination polymer is obtained by the reaction of Zn$(OH)_2$ and H_2oFBPDC in acetone with a small additive of water at 40 °C.

All previously mentioned Zn complexes have non-polymeric, 1D and 2D polymeric structure because of low coordination number of Zn(II) cation (4 and 5) and/or a large amount of the coordinated solvent molecules. The metal complex can have 3D polymeric structure when Zn(II) cation is coordinated with one or two solvent molecules or bridging N-donor co-ligand. Indeed, [Zn_2(H_2O)$_{1.5}$(thf)$_{1.5}$(oFBPDC)$_2$] · 3.5H_2O · 2.5THF [25], in which each Zn(II) cation is in a distorted octahedral environment, has a 3D polymeric structure with lozenge-shaped channels occupied with guest molecules of water and THF. The tendency to form layered coordination polymers based on Zn paddle wheel units has inspired us to implement a "pillaring strategy" in order to obtain 3D structures. Heating the stoichiometric mixture of Zn$(OH)_2$, H_2oFBPDC and dabco in methanol at 80 °C for 2 days afford 3D doubly interpenetrated framework [Zn_2(dabco)(oFBPDC)$_2$] · 4.5CH_3OH [25]. Paddle wheel secondary building units {Zn_2(RCO_2)$_4$L} form the same layers as in the layered complexes [Zn_2(CH_3CONH_2)$_2$(oFBPDC)$_2$] · 3CH_3CN, [Zn_2(CH_3CN)$_2$(oFBPDC)$_2$] · 2C_6H_6 · 2CH_3CN, and [Zn_2(H_2O)$_2$(oFBPDC)$_2$] · 4CH_3COCH_3. These layers are connected by dabco as pillars to form potentially porous framework. It is remarkable that changing dabco by bpy ligand does not lead to the isoreticular structure. Heating the suspension of Zn$(OH)_2$, H_2oFBPDC and bpy in water at 80 °C gives the crystals of compound (H_2bpy)[Zn_2(bpy)(oFBPDC)$_3$] (Fig. 3) [25] with 3D five-fold interpenetrated, and therefore non-porous, structure. The framework is anionic, its negative charge is balanced with H_2bpy^{2+} cations.

An analysis of crystal structures of Zn complexes containing oFBPDC^{2-} and BPDC^{2-} reveals that there are no isostructural complexes. There is no any information about BPDC^{2-} complexes in which Zn(II) cation is additionally coordinated with methanol, THF or acetonitrile because the syntheses of non-fluorinated PCPs usually take place in DMF, DMA or DMSO as solvents. The diffusion of triethylamine into the solution of Zn$(NO_3)_2$ · 6H_2O, H_2BPDC in DMSO results in layered coordination polymer [Zn_2(BPDC)$_2$(dmso)$_2$] · 4DMSO [34] with the same topology of the layers as in [Zn_2(CH_3CONH_2)$_2$(oFBPDC)$_2$] · 3CH_3CN, [Zn_2(CH_3CN)$_2$(oFBPDC)$_2$] · 2C_6H_6 · 2CH_3CN, and [Zn_2(H_2O)$_2$(oFBPDC)$_2$] · 4CH_3COCH_3. This demonstrates that the syntheses of non-fluorinated MOFs can take place in strongly coordinated solvents, while the formation of similar perfluorinated coordination polymers requires solvents with lower coordination ability.

Pillaring strategy works well in case of non-fluorinated and perfluorinated ligands and leads to 3D polymers [Cu_2(dabco)(BPDC)$_2$] [35] and [Cu_2(dabco)(oFBPDC)$_2$] (MOFF-2) [17], [Zn_2(dabco)(BPDC)$_2$] (DMOF-1-bpdc) [36] and [Zn_2(dabco)(oFBPDC)$_2$] [25]. Those frameworks have similar chemical composition and topology, but both fluorinated coordination polymers are doubly interpenetrated, unlike their non-fluorinated congeners.

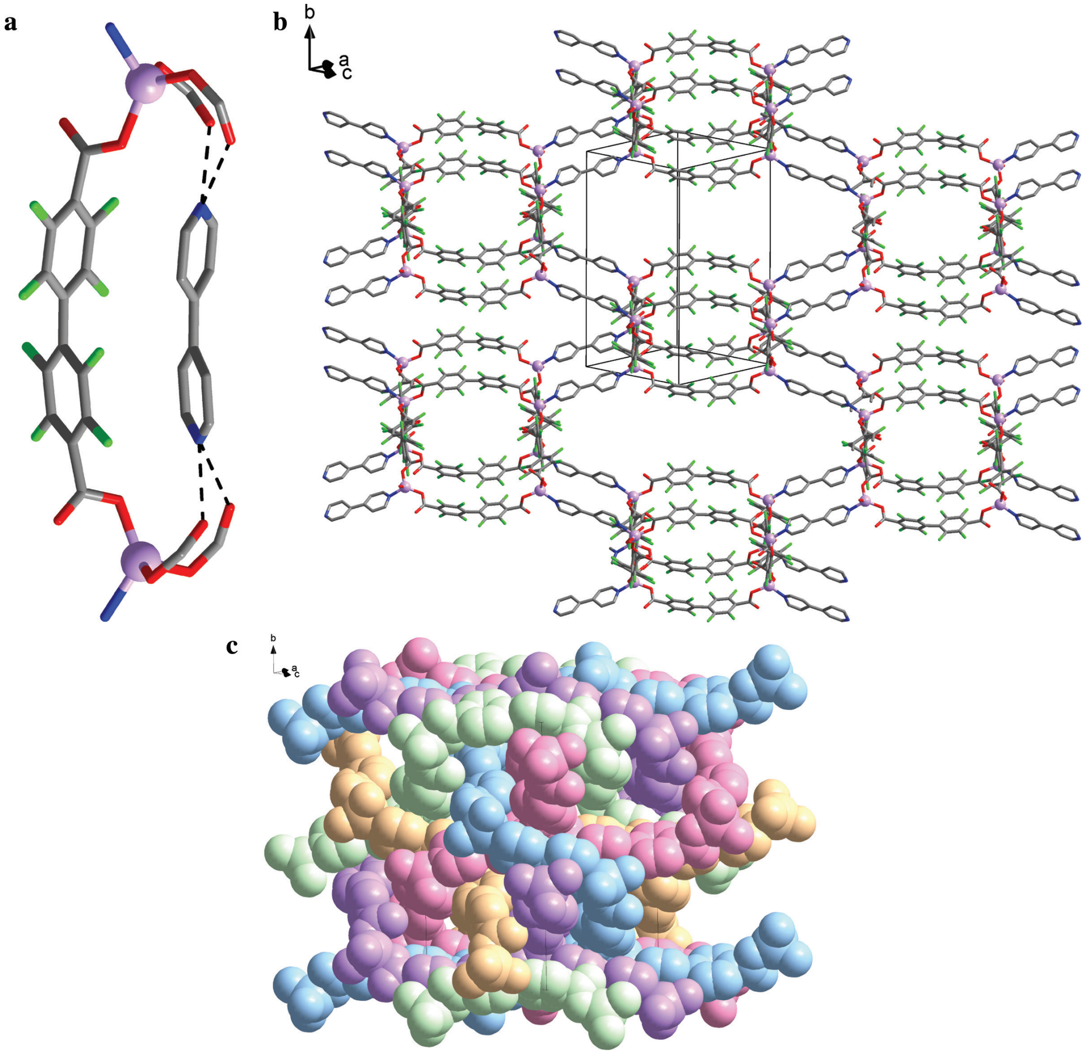

Fig. 3: (a) Coordination environment of Zn(II) cations in the structure of $(H_2bpy)[Zn_2(bpy)(oFBPDC)_3]$. Hydrogen atoms are omitted for clarity. Hydrogen bonds are shown with dashed lines. (b) The structure of one framework within the structure of five-fold interpenetrated $(H_2bpy)[Zn_2(bpy)(oFBPDC)_3]$. Hydrogen atoms and H_2bpy^{2+} cations are omitted for clarity. (c) Crystal packing of the metal-organic frameworks, showing five-fold interpenetration. H_2bpy^{2+} cations are omitted for clarity.

Non-fluorinated and perfluorinated aromatic carboxylic acids are different in reactivity and the coordination ability of their anions. The syntheses of metal complexes require different conditions, e.g. temperature, solvents, pH, etc. Isostructural non-fluorinated and perfluorinated MOFs mainly do not form. These circumstances make it difficult to compare the properties of such pairs of MOF and reveal the impact of fluorine atoms within an organic linker on the functionality of the resulted MOF. The only example of isostructural BPDC frameworks is Zr-UiO-67 [11] and Zr_6-oFBPDC described in 2018 by the group of Lin et al. [19]. Zr MOFs are famous for their outstanding chemical stability and high porosity, which make them promising material for catalysis, sorption and separation, drug delivery and sensing [37]. The perfluorinated version of UiO-67 is obtained by reacting $ZrOCl_2 \cdot 8H_2O$ with H_2oFBPDC in THF at 80 °C. EPR spectroscopy of MOF-bound $O_2^{\cdot-}$ and fluorescence spectroscopy of MOF-bound N-methylacridone have shown that Zr_6-oFBPDC is more Lewis acidic than nitrated MOF Zr_6-BPDC-$(NO_2)_2$ and non-modified UiO-67. The ligand perfluorination is a tool for enhancing Lewis acidity which is important for catalysis and sorption [19].

Crystal structures and sorption properties of oFBPDC-based MOFs

One of the most exciting features of MOFs is the presence of voids in their crystal structures after the removal of solvent guest molecules. In the case of oFBPDC based MOFs, these voids are decorated with highly electronegative fluorine atoms. Owing to the presence of fluorine atoms such MOFs are expected to have unique surface properties. The summary of porous oFBPDC based MOFs and their characteristics are presented in Table 2.

Layered Cu containing MOFF-1 (Fig. 4a) [17], $[Zn_2(CH_3CONH_2)_2(oFBPDC)_2] \cdot 3CH_3CN$ (Fig. 4b) [25], $[Zn_2(CH_3CN)_2(oFBPDC)_2] \cdot 2C_6H_6 \cdot 2CH_3CN$ (Fig. 4c) [20], and $[Zn_2(H_2O)_2(oFBPDC)_2] \cdot 4CH_3COCH_3$ (Fig. 4d) [20] have pretty similar polymeric layers and their packing. A distorted square grid layers are formed with binuclear paddle wheel units $\{M_2(RCO_2)_4L_2\}$ and $oFBPDC^{2-}$, with methanol, acetamide, acetonitrile or water acting as an apical ligand L. Activated MOFF-1 adsorbs *ca.* 165 cm^3/g of N_2 at 77 K, and its BET surface area is 580 m^2/g. Nitrogen uptakes at 77 K of activated Zn MOFs are significantly worse, however, they adsorb CO_2 at 195 K with BET surface areas of 151–470 m^2/g. Such differences can be explained by incomplete removal of coordinated acetamide and water molecules upon activation and packing of the layers in guest-free materials.

These layers are pillared with dabco to form doubly interpenetrated MOFF-2 [17] and $[Zn_2(dabco)(oFBPDC)_2]$ (Fig. 5) [25]. Both guest-free MOFs adsorb significant amounts of N_2 at 77 K with very close BET surface areas of 444 and 441 m^2/g, respectively. These are much lower than BET surface area of Cu non-fluorinated non-interpenetrated congener $[Cu_2(dabco)(BPDC)_2]$ (3625 m^2/g) [34], while its Zn analogue shows only 185 m^2/g [35]. $[Zn_2(dabco)(oFBPDC)_2]$ has been extensively investigated in terms of low-pressure gas and vapour sorption [25]. The uptake of CO_2 is larger than those for CH_4 and N_2 resulting in IAST selectivity factors CO_2 vs. N_2 and CO_2 vs. CH_4 11.3 and 4.9 at 273 K and 7.6 and 4.1 at 298 K, respectively, showing a moderate degree of selectivity. The heat of CO_2 adsorption at zero coverage is 23.4 kJ/mol, which is the evidence of the absence of strong binding sites within the MOF structure. The pore size of *ca.* 7 Å allows the MOF to adsorb and separate larger molecules such as C6 hydrocarbons. Indeed, benzene uptake at 293 K is more than 2 times higher than that of cyclohexane resulting in IAST selectivity factor benzene/cyclohexane more than 6 in all range of the compositions. A great advantage of $[Zn_2(dabco)(oFBPDC)_2]$ is the hydrophobicity of its internal surface and the stability in water vapours which is confirmed by water vapour sorption measurements followed by IR-spectroscopy and PXRD.

The sorption properties of Zr_6-oFBPDC [19] are of special interest because it is an isostructural analogue of highly porous UiO-67 (Fig. 6). In their inorganic building block, Zr(IV) atoms are located in the vertices of octahedron capped with μ_3-O and μ_3-OH groups. The coordination number of Zr(IV) is completed to 8 by four oxygen atoms of the bridging carboxylic group. This results in a 12-connected node $Zr_6(\mu_3\text{-}O)_4(\mu_3\text{-}OH)_4(RCO_2)_{12}$. These Zr_6 units are connected with bridging biphenyl-4,4′-dicarboxylate $BPDC^{2-}$ or its perfluorinated version

Table 2: The summary of porous oFBPDC-based MOFs and their characteristics.

MOF	Dimensionality	Gas, T	Volume adsorbed (STP), cm^3/g	S(BET), m^2/g
MOFF-1 $[Cu_2(CH_3OH)_2(oFBPDC)_2] \cdot 2CH_3OH$	2D	N_2, 77 K	*ca.* 165	580
$[Zn_2(CH_3CONH_2)_2(oFBPDC)_2] \cdot 3CH_3CN$	2D	N_2, 77 K	10.4	17.4
		CO_2, 195 K	97.8	470
$[Zn_2(CH_3CN)_2(oFBPDC)_2] \cdot 2C_6H_6 \cdot 2CH_3CN$	2D	N_2, 77 K	15.7	43.4
		CO_2, 195 K	88.8	335
$[Zn_2(H_2O)_2(oFBPDC)_2] \cdot 4CH_3COCH_3$	2D	CO_2, 195 K	44.6	151
MOFF-2 $[Cu_2(dabco)(oFBPDC)_2]$	3D	N_2, 77 K	*ca.* 125	444
$[Zn_2(dabco)(oFBPDC)_2] \cdot 4.5CH_3OH$	3D	N_2, 77 K	138.4	441
Zr_6-oFBPDC $Zr_6O_4(OH)_4(oFBPDC)_{4.27}[(OH)(OH_2)]_{3.46}$	3D	N_2, 77 K	*ca.* 380	1148

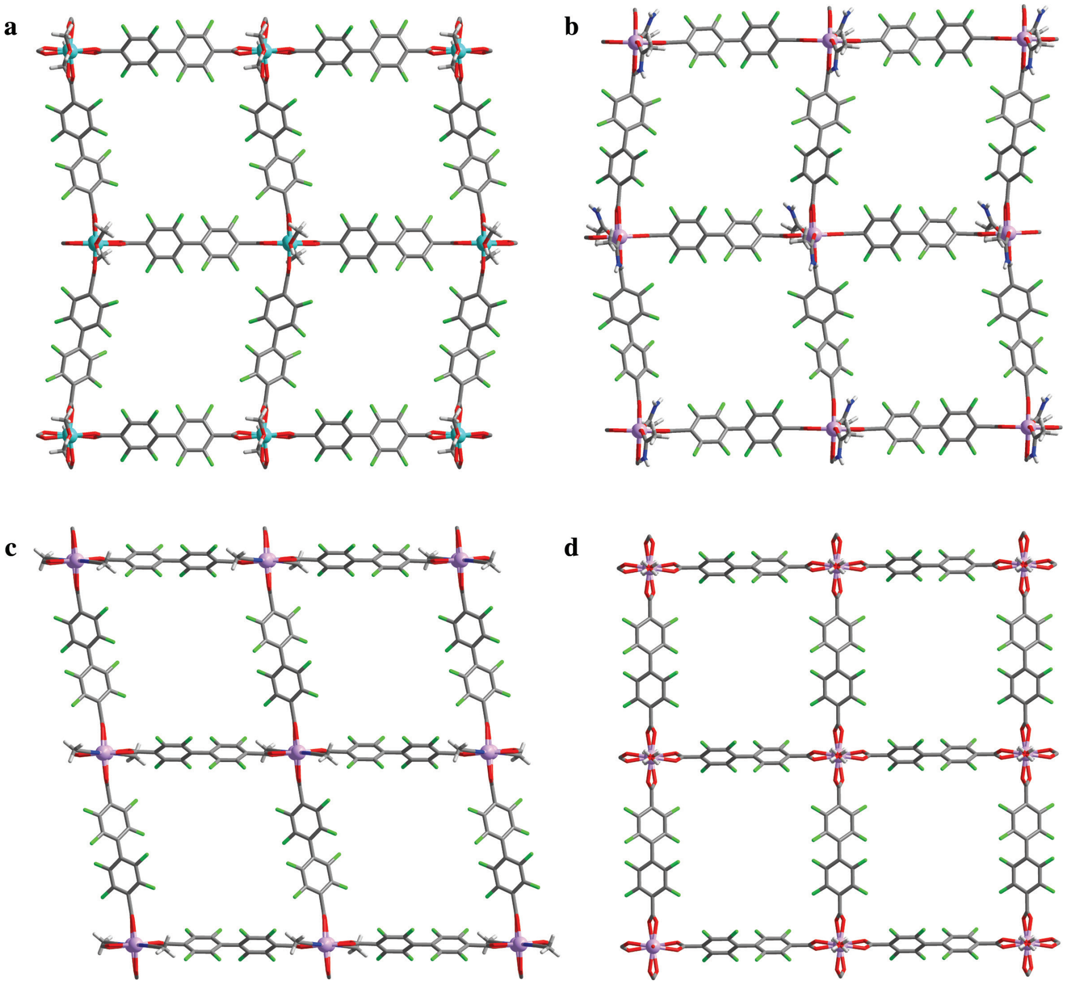

Fig. 4: The fragments of the polymeric layers of $[Cu_2(CH_3OH)_2(oFBPDC)_2] \cdot 2CH_3OH$ (MOFF-1) (a), $[Zn_2(CH_3CONH_2)_2(oFBPDC)_2] \cdot 3CH_3CN$ (b), $[Zn_2(CH_3CN)_2(oFBPDC)_2] \cdot 2C_6H_6 \cdot 2CH_3CN$ (c), and $[Zn_2(H_2O)_2(oFBPDC)_2] \cdot 4CH_3COCH_3$ (d). Guest molecules of methanol, acetonitrile, benzene and acetone are omitted for clarity.

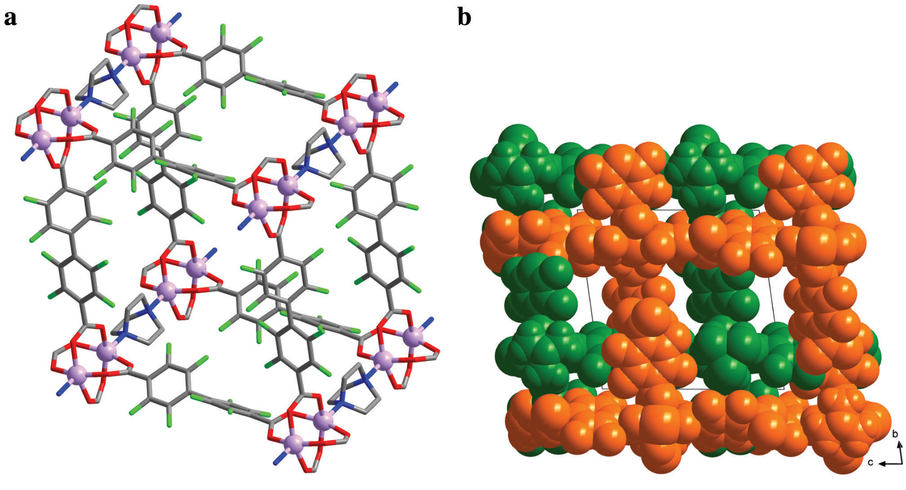

Fig. 5: (a) Fragment of the crystal structure of $[Zn_2(dabco)(oFBPDC)_2]$ showing the pillaring of the distorted square grid layers with dabco. (b) Crystal packing of doubly interpenetrated $[Zn_2(dabco)(oFBPDC)_2]$.

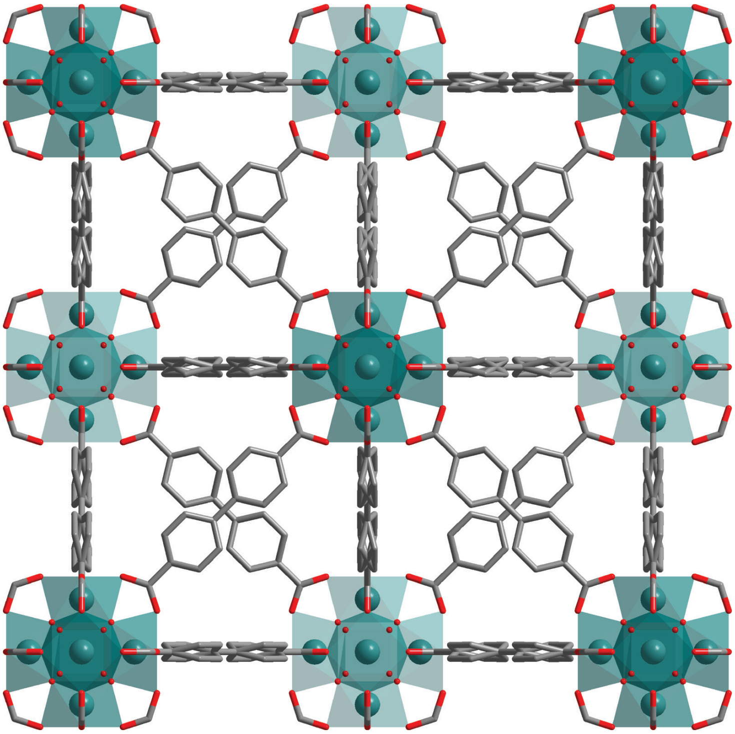

Fig. 6: Crystal structure of non-modified UiO-67. Hydrogen atoms are omitted for clarity.

forming a face-centred cubic lattice with tetrahedral and octahedral pores (Fig. 6). Depending on the method of synthesis, activation procedure and the presence of defects UiO-67 samples show BET surface areas of 2300–2600 m^2/g [38–42]. Zr_6-oFBPDC adsorbs less amount of N_2 at 77 K with BET surface area of 1148 m^2/g. The decrease in sorption capacity of perfluorinated frameworks is presumably due to larger framework density and reduced void volume. There is no information on sorption properties toward other gases as well as vapours. Our investigation of sorption properties of fluorinated and non-fluorinated UiO-67 toward different gases and vapours is underway.

Conclusion and perspectives

Ligand modification of an organic bridging ligand can impart a wide range of certain functionalities to a MOF material. Nevertheless, such modification in case of fully fluorinated aromatic carboxylic acids significantly changes the reactivity of the acid and crystal structures of the resulting MOFs. For these reasons, isostructural non-fluorinated and perfluorinated MOFs are very rare. On the other hand, the use of perfluorinated ligands allows one to obtain unique and unprecedented structures. Though the investigation of oFBPDC metal complexes is presented only in 6 papers, the functional properties of these complexes do demonstrate the importance of further investigation of such materials, including synthesis of new MOFs based on other metals (aluminium, iron, chromium, scandium, lanthanides, titanium, cerium(IV)) and detailed investigation of their functional properties such as selectivity of sorption and hydrophobicity, luminescence and catalytic activity.

Acknowledgements: Our study of MOFs based on perfluorinated dicarboxylates is carried out within the projects of Russian Foundation for Basic Research together with the Government of Novosibirsk region (funder id: http://dx.doi.org/10.13039/501100002261, No. 18-43-543028), Scholarship of President of Russian Federation (SP-3226.2019.1), and Russian Science Foundation (funder id: http://dx.doi.org/10.13039/501100006769, No 19-73-20087).

References

[1] P. Silva, S. M. F. Vilela, J. P. C. Tome, F. A. Almeida Paz. *Chem. Soc. Rev.* **44**, 6774 (2015).

[2] V. F. Cheong, P. Y. Moh. *Mater. Sci. Technol.* **34**, 1025 (2018).

[3] S. Yuan, L. Feng, K. Wang, J. Pang, M. Bosch, C. Lollar, Y. Sun, J. Qin, X. Yang, P. Zhang, Q. Wang, L. Zou, Y. Zhang, L. Zhang, Y. Fang, J. Li, H.-C. Zhou. *Adv. Mater.* **30**, 1704303 (2018).

[4] L. Jiao, J. Y. R. Seow, W. S. Skinner, Z. U. Wang, H.-L. Jiang. *Mater. Today* **27**, 43 (2019).

[5] S. Ali Akbar Razavi, A. Morsali. *Coord. Chem. Rev.* **399**, 213023 (2019).

[6] M. Eddaoudi, J. Kim, N. Rosi, D. Vodak, J. Wachter, M. O'Keeffe, O. M. Yaghi. *Science* **295**, 469 (2002).

[7] C. Serre, F. Millange, C. Thouvenot, M. Noguès, G. Marsolier, D. Louër, G. Férey. *J. Am. Chem. Soc.* **124**, 13519 (2002).

[8] G. Férey, C. Serre, C. Mellot-Draznieks, F. Millange, S. Surblé, J. Dutour, I. Margiolaki. *Angew. Chem.* **116**, 6456 (2004).

[9] G. Férey, C. Mellot-Draznieks, C. Serre, F. Millange, J. Dutour, S. Surblé, I. Margiolaki. *Science* **309**, 2040 (2005).

[10] T. Loiseau, C. Volkringer, M. Haouas, F. Taulelle, G. Férey. *Comptes Rendus Chim.* **18**, 1350 (2015).

[11] J. H. Cavka, S. Jakobsen, U. Olsbye, N. Guillou, C. Lamberti, S. Bordiga, K. P. Lillerud. *J. Am. Chem. Soc.* **130**, 13850 (2008).

[12] B. Chen, Y. Yang, F. Zapata, G. Qian, Y. Luo, J. Zhang, E. B. Lobkovsky. *Inorg. Chem.* **45**, 8882 (2006).

[13] D.-S. Zhang, Z. Chang, Y.-F. Li, Z.-Y. Jiang, Z.-H. Xuan, Y.-H. Zhang, J.-R. Li, Q. Chen, T.-L. Hu, X.-H. Bu. *Sci. Rep.* **3**, 3312 (2013).

[14] M. D. Defuria, M. Zeller, D. T. Genna. *Cryst. Growth Des.* **16**, 3530 (2016).

[15] S. Noro, T. Nakamura. *Npg Asia Mater.* **9**, e433 (2017).

[16] P. Pachfule, R. Banerjee. Metal-organic frameworks: fluorinated frameworks, in *Encyclopedia of Inorganic and Bioinorganic Chemistry*, R. A. Scott (Ed.), John Wiley & Sons, Ltd., Hoboken, NJ, USA (2014).

[17] T.-H. Chen, I. Popov, O. Zenasni, O. Daugulis, O. Š. Miljanić. *Chem. Commun.* **49**, 6846 (2013).

[18] S. V. Larionov, L. I. Myachina, L. A. Sheludyakova, I. V. Korolkov, M. I. Rakhmanova, P. E. Plyusnin, A. S. Vinogradov, V. M. Karpov, V. E. Platonov, V. P. Fadeeva. *Russ. J. Gen. Chem.* **85**, 1617 (2015).

[19] P. Ji, T. Drake, A. Murakami, P. Oliveres, J. H. Skone, W. Lin. *J. Am. Chem. Soc.* **140**, 10553 (2018).

[20] A. M. Cheplakova, K. A. Kovalenko, D. G. Samsonenko, A. S. Vinogradov, V. M. Karpov, V. E. Platonov, V. P. Fedin. *CrystEngComm*. **21**, 2524 (2019).

[21] D. Jiang, A. D. Burrows, K. J. Edler. *CrystEngComm.* **13**, 6916 (2011).

[22] Y. H. Huang, W. S. Lo, Y. W. Kuo, W. J. Chen, C. H. Lin, F. K. Shieh. *Chem. Commun.* **53**, 5818 (2017).

[23] Z. Hulvey, J. D. Furman, S. A. Turner, M. Tang, A. K. Cheetham. *Cryst Growth Des.* **10**, 2041 (2010).

[24] S. V. Larionov, M. I. Rakhmanova, L. A. Glinskaya, D. Yu. Naumov, A. S. Vinogradov, V. M. Karpov, V. E. Platonov, V. P. Fadeeva. *Russ. J. Gen. Chem.* **89**, 261 (2019).

[25] A. M. Cheplakova, K. A. Kovalenko, D. G. Samsonenko, V. A. Lazarenko, V. N. Khrustalev, A. S. Vinogradov, V. M. Karpov, V. E. Platonov, V. P. Fedin. *Dalton Trans*. **47**, 3283 (2018).

[26] S. A. Sapchenko, D. N. Dybtsev, V. P. Fedin. *Pure Appl. Chem.* **89**, 1049 (2017).

[27] S. Jin, H. Zhang, K. Xu, X. Ye, Y. Zhang, Y. Fang, D. Wang. *Polyhedron* **95**, 108 (2015).

[28] J. Krautwurst, D. Smets, R. Lamann, U. Ruschewitz. *Inorg. Chem.* **58**, 8622 (2019).

[29] A. Cheplakova, D. Samsonenko, *CSD Commun.* (2019), DOI: 10.5517/ccdc.csd.cc2280s5.

[30] A. M. Cheplakova, D. G. Samsonenko, V. P. Fedin. *J. Struct. Chem*. **60**, 289 (2019).

[31] H. M. M. Shearer, C. B. Spencer. *Chem. Commun.* 194a (1966). https://pubs.rsc.org/en/content/articlelanding/1966/C1/c1966000194a#!divAbstract.

[32] J. M. Burlitch, S. E. Hayes, G. E. Whitwell. *Organometallics* **1**, 1074 (1982).

[33] S. Jana, R. J. F. Berger, R. Fröhlich, T. Pape, N. W. Mitzel. *Inorg. Chem.* **46**, 4293 (2007).

[34] J. Tao, X. Yin, R. Huang, L. Zheng, S. Weng Ng. *Inorg. Chem. Commun.* **5**, 975 (2002).

[35] K. Seki. *Chem. Commun.* 1496 (2001). https://pubs.rsc.org/en/content/articlelanding/2001/CC/b104204c#!divAbstract.

[36] P. V. Dau, M. Kim, S. J. Garibay, F. H. L. Münch, C. E. Moore, S. M. Cohen. *Inorg. Chem.* **51**, 5671 (2012).

[37] Y. Bai, Y. Dou, L.-H. Xie, W. Rutledge, J.-R. Li, H.-C. Zhou. *Chem. Soc. Rev.* **45**, 2327 (2016).

[38] M. J. Katz, Z. J. Brown, Y. J. Colón, P. W. Siu, K. A. Scheidt, R. Q. Snurr, J. T. Hupp, O. K. Farha. *Chem. Commun.* **49**, 9449 (2013).

[39] J. H. Cavka, C. A. Grande, G. Mondino, R. Blom. *Ind. Eng. Chem. Res.* **53**, 15500 (2014).

[40] N. Ko, J. Hong, S. Sung, K. E. Cordova, H. J. Park, J. K. Yang, J. Kim. *Dalton Trans.* **44**, 2047 (2015).

[41] K. Leus, T. Bogaerts, J. De Decker, H. Depauw, K. Hendrickx, H. Vrielinck, V. Van Speybroeck, P. Van Der Voort. *Microporous Mesoporous Mater.* **226**, 110 (2016).

[42] S. Øien-Ødegaard, B. Bouchevreau, K. Hylland, L. Wu, R. Blom, C. Grande, U. Olsbye, M. Tilset, K. P. Lillerud. *Inorg. Chem.* **55**, 1986 (2016).